NASA TR R-121

NATIONAL AERONAUTICS AND SPACE ADMINISTRATION

TECHNICAL REPORT
R-121

A THEORETICAL STUDY OF THE MOTION OF AN IDEALIZED PLASMA RING UNDER THE INFLUENCE OF VARIOUS COAXIAL MAGNETIC FIELDS

By CLARENCE W. MATTHEWS

1961

For sale by the Superintendent of Documents, U.S. Government Printing Office, Washington 25, D.C. Yearly subscription, $15; foreign, $19; single copy price varies according to size ---------- Price 30 cents

Code 1

SINGLE COPY ONLY

TECHNICAL REPORT R-121

A THEORETICAL STUDY OF THE MOTION OF AN IDEALIZED PLASMA RING UNDER THE INFLUENCE OF VARIOUS COAXIAL MAGNETIC FIELDS

By CLARENCE W. MATTHEWS

Langley Research Center
Langley Air Force Base, Va.

TECHNICAL REPORT R-121

A THEORETICAL STUDY OF THE MOTION OF AN IDEALIZED PLASMA RING UNDER THE INFLUENCE OF VARIOUS COAXIAL MAGNETIC FIELDS

By Clarence W. Matthews

SUMMARY

14873

The equations of motion of charged particles in a magnetic field have been applied to the problem of the motion of an idealized plasma ring in the magnetic fields arising from direct and/or alternating current flowing through a set of coaxial drive coils. The simplifications involved are such that the theory predicts the maximum velocities obtainable with the induced-electromotive-force plasma accelerator.

For the single-coil induced-electromotive-force plasma accelerator the maximum axial velocities attained can be expressed by two simple empirical equations, one for small velocities and the other for large velocities, provided the constants are originally determined by applicable data.

The results of a preliminary survey of multicoil traveling-wave accelerators indicate that such accelerators have very exacting design requirements if the plasma ring is to be contained within the accelerator throughout the entire process.

INTRODUCTION

The single-coil induced-electromotive-force accelerator is often referred to in the literature as an electromagnetic shock tube. In many studies, such as those of references 1 to 3, the accelerator is used to produce a fast hot shock front for the purpose of the introduction of plasma into various fusion machines. In other studies (for example, ref. 4) this type of accelerator is used to produce a hot fast flow over a blunt magnetized body. An experimental analysis, in which the formation of the shock front was studied (ref. 5), showed that the induced-electromotive-force plasma accelerator was capable of producing appreciably higher velocities than were observed in the leading shock front. In this analysis it was suggested that a theoretical study be made to indicate the maximum capabilities and other characteristics of induced-electromotive-force plasma accelerators.

This goal was achieved by applying the theoretical equations of motion of charged particles in a magnetic field to a distribution of equal numbers of electrons and singly charged positive ions in the magnetic field of a sinusoidal current flowing through a coaxial drive coil. The simplifications involved in the present study, such as disregarding effects of collisions, pressure gradients, space charges, and partial ionization, were such that the theory must necessarily predict the optimum velocities attainable in the idealized accelerator.

The purpose of this paper is to present the results of the application of this simplified theory to several coil configurations. The variations in the velocity due to variation of atomic weight of the ions composing the plasma and to numbers of ions in the ring are also presented.

SYMBOLS

The rationalized mksq system of units is used herein.

$\mathbf{A}$	magnetic vector potential
A_θ	azimuthal component of $\mathbf{A}$
A	used for A_θ
a	minor radius of plasma ring
B	nondimensional drive intensity factor, $\mu_0 Ie/4\pi m\omega r_{max}$
C, C_1, C_2, D	constants
E	complete elliptic integral of second kind
e	charge on singly charged positive ion
f	frequency of alternating component of drive current
I	maximum value of $i_{ac,m}$
i	instantaneous drive current
K	complete elliptic integral of first kind

k_1, k_2 constants; see appendix A
$d\mathbf{l}$ vector differential element
L Lagrangian
L_2 self-inductance of plasma ring
m mass of single electron
m_q mass of a number of uniformly charged particles
n number of electrons or of ions in plasma ring
P potential function other than electric or magnetic
q charge of electricity
$\mathbf{R}$ position vector of a point in space
r radial coordinate of a point in a cylindrical system
r_{max} base length for nondimensionalization, considered for this study to be maximum drive-coil radius
$\mathbf{r}_o$ unit radial vector
S number of turns in drive coil
t time
V potential function due to electrostatic fields
x axial coordinate of a point in a cylindrical system
$\mathbf{x}_o$ unit axial vector
$\alpha_m = -4\pi^2 M_m/\mu_o i_m$
β ratio of ion mass to electron mass
γ nondimensional current, i/I
δ_m phase angle of alternating current in mth turn of drive coil
$\zeta = \mu\mu_o n e^2/4\pi^2 m r_{max}$
θ azimuthal coordinate of a point in a cylindrical system
$\boldsymbol{\theta}_o$ unit azimuthal vector
$\mu = L_2 = \mu\mu_o r$
μ_o permeability of free space, $4\pi \times 10^{-7}$ henry/m
$\nu_m = \rho_m^2 + \rho^2 + (\chi - \chi_m)^2$
$\xi_m = 2\rho_m\rho$
ρ nondimensional radial coordinate, r/r_{max}
τ nondimensional time coordinate, ωt
ϕ nondimensional azimuthal coordinate (equivalent to θ)
χ nondimensional axial coordinate, x/r_{max}
ω angular drive frequency, $2\pi f$, radians per second

Subscripts:

ac alternating current, maximum value
D quantity associated with all turns of drive coil
dc magnitude of direct-current component
e quantity associated with electrons of plasma
i quantity associated with ions of plasma
m mth turn of drive-coil system
0 starting condition of plasma ring

A bold face symbol indicates a vector quantity.

Dots over symbols indicate differentiation with respect to t or to τ if over a nondimensional variable.

THEORY

An induced-electromotive-force plasma accelerator consists essentially of two coupled coils similar to an air-core transformer. One of these coils is the drive coil which is excited by a large high-frequency alternating current. The resultant changing magnetic field sets up an induced voltage gradient in the neighborhood of the coil that is capable, provided the gas in this region is within the proper pressure range, of causing an arc to form in the magnetic field. If the drive coil is circular, this arc creates a circular plasma ring coaxial with the drive coil. Since currents are flowing in both coils, a force reaction exists between the drive coil and the plasma ring because of the interacting magnetic fields. This force is the one which can be used to accelerate the plasma ring to high axial velocities.

The properties of this coaxial system are considered in this paper. Schematic diagrams of a coaxial coil accelerator and the coordinate system used are shown in figures 1(a) and 1(b).

METHOD OF ANALYSIS

An analysis of the motion of the plasma ring can be undertaken in several ways. One way is to use the force relations between the magnetic fields of the drive coil and the plasma ring. In this method, however, it is difficult to account for the fact that the ring consists of moving charged particles which create the current flowing in the plasma. Another method is to apply the equations of motion of a group of charged particles in a magnetic field to the problem of a neutral plasma ring moving in the field of a coaxial coil. Before these equations are presented, however, several simplifying assumptions can be made

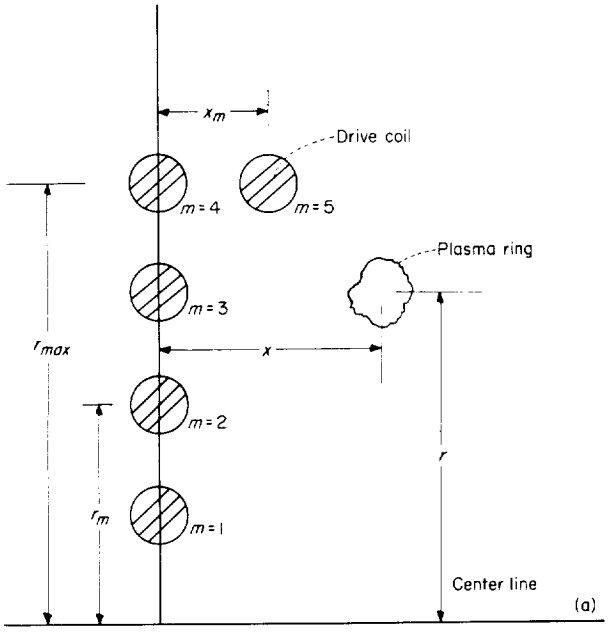

(a) Plasma ring and coil-turn notation.

FIGURE 1.—Schematic diagram of an induced-electromotive-force plasma accelerator and the cylindrical coordinate system used in this investigation.

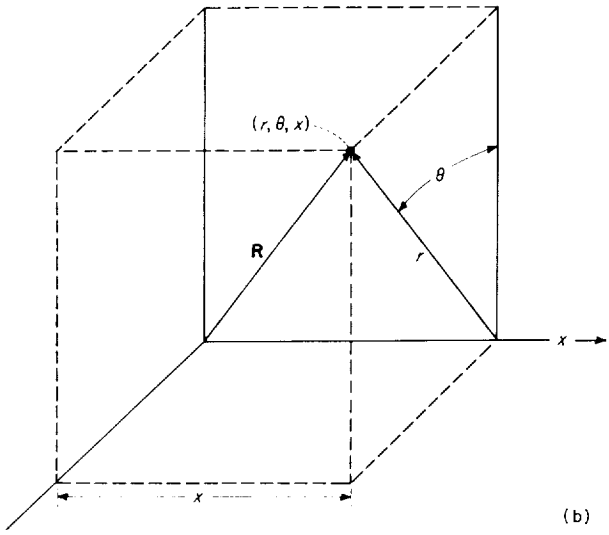

(b) Coordinate system.

FIGURE 1.—Concluded.

concerning the nature of the plasma.

In order to avoid studies of the effects of collisions, it is assumed that the plasma is both fully ionized and at a sufficiently high temperature, so that the resistance of the ring is small compared with its inductive reactance. As a result, the resistance of the plasma ring may be neglected. The assumption is also made that the plasma ring moves through a vacuum; thus, pressure does not affect the motion of the ring, and the potential due to pressure may be assumed to be zero. The plasma ring is additionally assumed to be neutral in charge; that is, it is composed of a number of singly charged positive ions and an equal number of electrons. Also, the ions and electrons are assumed to form only one ring because of the large electrical forces existing between the particles. With these assumptions in mind, consider the application of the equations of motion of charged particles to the analysis of the induced-electromotive-force plasma accelerator.

EQUATIONS OF MOTION OF A PLASMA RING

The Lagrangian of the motion of a mass m_q, having a charge q, under the influence of a magnetic field is given on page 347 of reference 6 as

$$L=\frac{1}{2}m_q\dot{\mathbf{R}}\cdot\dot{\mathbf{R}}+q\dot{\mathbf{R}}\cdot\mathbf{A}-P-qV \qquad (1)$$

where

$\dot{\mathbf{R}}$	velocity $d\mathbf{R}/dt$ of the mass
$\mathbf{A}$	magnetic vector potential
V	electric potential field
P	any other potential

Since a mass of plasma must consist of an equal number of positive ions and electrons, equation (1) must be modified if it is to account for both groups of charged particles. This modification may be made by writing the Lagrangian for each set of particles and then adding the two functions. The $\mathbf{A}$ field arises from three different current loops—namely, the current in the drive coil, the current from the flow of electrons, and the current from the flow of ions. If the subscripts i and e are used to show that the indicated function is of ion or electron origin, then the magnetic vector potential $\mathbf{A}$ may be written $\mathbf{A}_D+\mathbf{A}_i+\mathbf{A}_e$ where $\mathbf{A}_D$ indicates the vector potential of the current flowing in the drive coil. With the use of this value of $\mathbf{A}$, the Lagrangian of the plasma may be written as

$$L=\frac{1}{2}m_i\dot{\mathbf{R}}_i\cdot\dot{\mathbf{R}}_i+\frac{1}{2}m_e\dot{\mathbf{R}}_e\cdot\dot{\mathbf{R}}_e+q_i\dot{\mathbf{R}}_i\cdot(\mathbf{A}_D+\mathbf{A}_i+\mathbf{A}_e)$$
$$+q_e\dot{\mathbf{R}}_e\cdot(\mathbf{A}_D+\mathbf{A}_i+\mathbf{A}_e)-P_i-P_e-q_iV_i-q_eV_e \qquad (2)$$

Several of the basic assumptions may now be

applied to equation (2). First, the assumption is made that gravitational and pressure effects are so small, compared with the magnetic effects, as to be negligible. Thus, both P_i and P_e are considered to be zero. The assumed condition that the average radial and axial coordinates of the ion and electron rings are the same may be expressed by $r_i=r_e=r$ and $x_i=x_e=x$.

Another simplification arises from the fact that only drive coils with coaxial circular turns are considered. This condition simplifies the vector $\mathbf{A}_D$ by eliminating the r- and x-components with only the θ-component A_θ remaining, as may be seen by examination of the following integral used to evaluate $\mathbf{A}$ due to current i in a coil (ref. 6, p. 315):

$$\mathbf{A}=\frac{\mu_o i}{4\pi}\oint\frac{d\mathbf{l}}{|\mathbf{R}-\mathbf{R}_m|} \tag{3}$$

where

μ_o	permeability of free space
$d\mathbf{l}$	a differential element of the coil
$\mathbf{R}$	position vector of a point in space
$\mathbf{R}_m$	position vector of $d\mathbf{l}$

For a coaxial coil $d\mathbf{l}=r_m d\theta\boldsymbol{\theta}_o$, where $\boldsymbol{\theta}_o$ is the unit azimuthal vector. Integration of equation (3) around the coil leads to a resultant vector in the azimuthal direction $\boldsymbol{\theta}_o$ for the field point concerned. Thus,

$$\mathbf{A}_D=A_D(r,x)\boldsymbol{\theta}_o$$

Since the induced electromotive forces which accelerate the charged particles are proportional to $\partial\mathbf{A}/\partial t$, where t is the time, the initial motion of the plasma is in the direction of the azimuthal vector, or the plasma tends to move in circles concentric with the drive coil. Also, evaluation of equation (3) shows that $A_{\theta,D}$ is not a function of θ; hence, each plasma particle is subject to the same electromotive force regardless of its angular location. As a result the plasma may be considered to be uniformly distributed about a ring.

Since the space charges can be assumed to hold the two plasma-ring components together so tightly that the relative motions in the r- and x-directions are small, the effects of the electrostatic potentials V_e and V_i may be neglected in any treatment of the overall motion.

Several simplifying relations are now required to reduce equation (2) to a more useful form. Since

$$\mathbf{A}_D=A_D\boldsymbol{\theta}_o \tag{4}$$

and the ions and electrons create an azimuthal current only—that is, they flow oppositely about the ring but together in the r- and x-directions—their corresponding magnetic vector potentials are similar to that of the drive coil, so that

$$\mathbf{A}_i=A_i\boldsymbol{\theta}_o \tag{5}$$

and

$$\mathbf{A}_e=A_e\boldsymbol{\theta}_o \tag{6}$$

For simplicity, the subscript θ has been dropped from the terms $A_{\theta,D}$, $A_{\theta,i}$, and $A_{\theta,e}$. Also, in terms of cylindrical coordinates,

$$\dot{\mathbf{R}}=\dot{r}\mathbf{r}_o+r\dot{\theta}\boldsymbol{\theta}_o+\dot{x}\mathbf{x}_o \tag{7}$$

where $\mathbf{r}_o$, $\boldsymbol{\theta}_o$, and $\mathbf{x}_o$ are the unit radial, azimuthal, and axial vectors, respectively, and the dots over the symbols indicate the first derivative with respect to time t.

Substitution of equations (4) to (7) into equation (2) gives the Lagrangian of the plasma ring as

$$L=\frac{1}{2}(m_i+m_e)(\dot{r}^2+\dot{x}^2)+\frac{1}{2}r^2(m_i\dot{\theta}_i^2+m_e\dot{\theta}_e^2)$$

$$+(q_i r\dot{\theta}_i+q_e r\dot{\theta}_e)(A_D+A_i+A_e) \tag{8}$$

The two terms $q_i r\dot{\theta}_i A_i$ and $q_e r\dot{\theta}_e A_e$ involve the determination of A_i and A_e within the plasma ring. These computations require a volume form of the integral in equation (3) in which the current density distribution is known throughout the cross section of the ring. The magnitude of the vector potential $\mathbf{A}$ may be evaluated with the following equation (from ref. 6, p. 324):

$$U=\frac{L_2 i^2}{2}=\frac{1}{2}\oint i\mathbf{A}\cdot d\mathbf{l}$$

where U is the energy stored in the magnetic field and L_2 is the self-inductance of the plasma ring. In this study $\mathbf{A}=A\boldsymbol{\theta}_o$ and $d\mathbf{l}=r d\theta\boldsymbol{\theta}_o$. Thus, A may be related to the inductance as follows:

$$\frac{L_2 i^2}{2}=\frac{i}{2}Ar\oint\boldsymbol{\theta}_o\cdot\boldsymbol{\theta}_o d\theta=\pi rAi \tag{9}$$

The values of the two currents in the plasma ring

may be expressed as

$$i_i=\frac{q_i\dot{\theta}_i}{2\pi}$$

and

$$i_e=\frac{q_e\dot{\theta}_e}{2\pi}$$

The substitution of these current values into equation (9) results in the following values of A_i and A_e for the ion and electron flows, respectively:

$$\left.\begin{aligned}A_i&=\frac{L_2q_i\dot{\theta}_i}{4\pi^2r}\\A_e&=\frac{L_2q_e\dot{\theta}_e}{4\pi^2r}\end{aligned}\right\}\qquad(10)$$

Substitution of the values of A_i and A_e from equations (10) into the Lagrangian (eq. (8)) results in

$$L=\frac{1}{2}(m_i+m_e)(\dot{r}^2+\dot{x}^2)+\frac{1}{2}m_ir^2\dot{\theta}_i^2+\frac{1}{2}m_er^2\dot{\theta}_e^2$$
$$+(q_i\dot{\theta}_i+q_e\dot{\theta}_e)rA_D+L_2\frac{(q_i\dot{\theta}_i+q_e\dot{\theta}_e)^2}{4\pi^2}\qquad(11)$$

Although this form of the Lagrangian may be substituted into Lagrange's equations to give the equation of motion of the plasma ring, it is more convenient to have the final equation of motion expressed in a nondimensional form, as such a form shows the various important parameters involved in the motion. The Lagrangian (eq. (11)) may be transformed into a nondimensional form with the use of the following relations.

Let m be the mass of a single electron and n the number of electrons or ions in the ring. Then,

$$\left.\begin{aligned}m_e&=nm\\m_i&=n\beta m\end{aligned}\right\}\qquad(12)$$

where β is the ratio of the ion mass to the electron mass. If $-e$ is the charge on a single electron and $+e$ the charge on a singly ionized positive ion, then

$$\left.\begin{aligned}q_e&=-ne\\q_i&=ne\end{aligned}\right\}\qquad(13)$$

The following relations are also used, in which χ, ρ, ϕ, and τ are the nondimensional variables:

$$\left.\begin{aligned}x&=\chi r_{max} & r&=\rho r_{max} & \theta&=\phi\\\dot{x}&=\frac{d\chi}{d\tau}\omega r_{max} & \dot{r}&=\frac{d\rho}{d\tau}\omega r_{max} & \dot{\theta}&=\frac{d\phi}{d\tau}\omega\\\ddot{x}&=\frac{d^2\chi}{d\tau^2}\omega^2r_{max} & \ddot{r}&=\frac{d^2\rho}{d\tau^2}\omega^2r_{max} & \ddot{\theta}&=\frac{d^2\phi}{d^2\tau}\omega^2\\\tau&=\omega t\end{aligned}\right\}\qquad(14)$$

The length r_{max} is any given characteristic length, considered in this paper to be the maximum drive-coil radius. The current flowing in the mth turn in the drive coil is nondimensionalized with the following substitution:

$$\gamma_m=\frac{i_m}{I}=\frac{i_{dc,m}+i_{ac,m}\sin(\tau-\delta_m)}{I}$$

in which $i_{dc,m}$ and $i_{ac,m}$ represent, respectively, the value of the direct current and the maximum value of the alternating current flowing in the mth turn, I is the maximum value of $i_{ac,m}$, and δ_m is the phase angle of the alternating current flowing in the mth turn.

Two nondimensional parameters appear in the process of nondimensionalization. These parameters may be conveniently referred to as B and ζ and are defined as follows:

$$B=\frac{\mu_0e}{4\pi m}\frac{I}{\omega r_{max}}=1.759\frac{I}{\omega r_{max}}\times10^4\qquad(15)$$

and

$$\zeta=\frac{\mu\mu_0ne^2}{4\pi^2mr_{max}}=\frac{0.910\mu n\times10^{-15}}{r_{max}}\qquad(16)$$

The value μ is defined by $L_2=\mu\mu_0r$. In a single-turn coil which defines the plasma ring

$$\mu=\log_e\frac{8r}{a}-1.75$$

(ref. 6, p. 330) where r is the major radius and a is the minor radius of the plasma ring. It is also convenient to convert A_m into a product of the instantaneous current and a function of position $\alpha_m(\rho,\chi)$; thus,

$$A_m=\frac{\mu_0i_m\alpha_m}{4\pi}=\frac{\mu_0I\gamma_m\alpha_m}{4\pi}$$

With this substitution, the magnitude of the magnetic vector potential due to the drive coils

may now be written

$$A_D=\frac{\mu_0 I}{4\pi}\sum_{m=1}^{S}\alpha_m\gamma_m \tag{17}$$

where the summation covers all turns of the drive coil. With the substitution of equations (12) to (17) into equation (11) and simplification, the Lagrangian L becomes in its nondimensional form L_{nd}, where the dot indicates differentiation with respect to τ,

$$L_{nd}=\frac{1+\beta}{2}(\dot\rho^2+\dot\chi^2)+\frac{\rho^2}{2}(\beta\dot\phi_i^2+\dot\phi_e^2)$$
$$+B(\dot\phi_i-\dot\phi_e)\rho\sum_{m=1}^{S}\alpha_m\gamma_m+\zeta\rho(\dot\phi_i-\dot\phi_e)^2 \tag{18}$$

The equations of motion of the plasma ring are now obtained by substituting L_{nd} into Lagrange's equations, which are, from reference 6, page 347,

$$\frac{d}{d\tau}\left(\frac{\partial L_{nd}}{\partial \dot z_i}\right)=\frac{\partial L_{nd}}{\partial z_i}$$

where z_i represents a generalized coordinate of Lagrange's equations.

If the coordinates ρ, χ, ϕ_e, and ϕ_i are substituted for z_i consecutively in Lagrange's equations, then the equations of motion of an idealized plasma ring may be written

$$(1+\beta)\ddot\rho-\rho(\beta\dot\phi_i^2+\dot\phi_e^2)-\zeta(\dot\phi_i-\dot\phi_e)^2$$
$$=B(\dot\phi_i-\dot\phi_e)\sum_{m=1}^{S}\gamma_m\frac{\partial(\rho\alpha_m)}{\partial\rho} \tag{19a}$$

$$(1+\beta)\ddot\chi=\rho B(\dot\phi_i-\dot\phi_e)\sum_{m=1}^{S}\gamma_m\frac{\partial\alpha_m}{\partial\chi} \tag{19b}$$

The equations for ϕ_e and ϕ_i may be integrated once and solved simultaneously for $\dot\phi_e$ and $\dot\phi_i$. The resultant equations are

$$\dot\phi_e=\frac{\beta\rho\left(C_e+\rho B\sum_{m=1}^{S}\alpha_m\gamma_m\right)+2\zeta(C_e+C_i)}{\rho^2[\beta\rho+2\zeta(1+\beta)]} \tag{19c}$$

$$\dot\phi_i=\frac{\rho\left(C_i-\rho B\sum_{m=1}^{S}\alpha_m\gamma_m\right)+2\zeta(C_e+C_i)}{\rho^2[\beta\rho+2\zeta(1+\beta)]} \tag{19d}$$

where the constants of integration C_e and C_i are

$$C_e=\rho_0\left[(\rho_0+2\zeta)\dot\phi_{e,0}-2\zeta\dot\phi_{i,0}-B\sum_{m=1}^{S}\alpha_{m,0}\gamma_{m,0}\right]$$

$$C_i=\rho_0\left[(\beta\rho_0+2\zeta)\dot\phi_{i,0}-2\zeta\dot\phi_{e,0}+B\sum_{m=1}^{S}\alpha_{m,0}\gamma_{m,0}\right]$$

The subscript zero indicates the value of the quantity at starting time.

The function α_m (or $4\pi A_m/\mu_0 i_m$) is obtained by integrating equation (3) over the mth turn of the drive coil. The values thus obtained for α_m and its derivatives are

$$\alpha_m=2\frac{\nu_m K_m-(\nu_m+\xi_m)E_m}{\rho(\nu_m+\xi_m)^{1/2}}$$

$$\frac{\partial\alpha_m}{\partial\chi}=\frac{2(\chi_m-\chi)[\nu_m E_m-(\nu_m-\xi_m)K_m]}{\rho(\nu_m+\xi_m)^{1/2}(\nu_m-\xi_m)}$$

$$\frac{\partial\alpha_m}{\partial\rho}=\frac{[\rho_m(2\nu_m^2-\xi_m^2)-\rho\nu_m\xi_m]E_m-(2\rho_m\nu_m-\rho\xi_m)(\nu_m-\xi_m)K_m}{\rho^2\rho_m(\nu_m+\xi_m)^{1/2}(\nu_m-\xi_m)}$$

where

$$\nu_m=[\rho_m^2+\rho^2+(\chi-\chi_m)^2]$$

and

$$\xi_m=2\rho\rho_m$$

The value of the argument of the complete elliptic functions K_m and E_m is

$$\left[\frac{4\rho\rho_m}{(\rho+\rho_m)^2+(\chi-\chi_m)^2}\right]^{1/2}$$

CALCULATIONS AND ASSUMPTIONS

An inspection of the equations of motion (19) of the plasma ring shows that they are nonlinear equations with complicated functions of the various coordinates. Although no proof can be presented, the equations appear to be of such a nature that only numerical solutions can be obtained. With this approach in mind, an analysis of the results is quite similar to setting up

various experiments in which exact control of all parameters is possible. For example, in the studies to be presented, the following controls are available: no collisions occur between the ions and electrons; the radial and axial components of the ion and electron paths coincide; the coil configuration and coil currents are controlled; and the starting time, initial location, and velocity of the ring are exactly determined. This method also allows exact determination of both the velocity and location of the ring. The numerical solutions were obtained by inserting equations (19) into an integration program used in an IBM 7090 electronic data processing system. The program used automatically adjusted the integration interval until a certain desired accuracy was obtained four significant figures for the computations presented in this paper.

The plasma rings for most of the conditions computed were considered to be made of equal numbers of hydrogen ions and electrons. Various coils (figs. 2(a) and (b)), coil combinations (figs. 2(c) to (e)), currents, and current combinations were used in the computations. Computations were made for the single-turn coil using an alternating drive current for values of the drive intensity factor B varying from 0.176 to 1,760,000 with ζ varying from 0.001 to 100. Most of these computations used starting conditions of $\chi_0=0.1$, $\rho_0=1.0$, and $\dot{\chi}_0=\dot{\rho}_0=\dot{\phi}_0=0$. Several of these calculations were also made for an additional steady current flowing through the drive coil.

Computations were made for two-coil, two-phase and for four-coil, two-phase traveling-wave systems with starting conditions similar to those previously given except that ρ_0 was equal to 0.75. A few computations were made for a coil combination similar to the "Scylla" fusion machine (ref. 3) to determine the possibilities of oscillations of the ring.

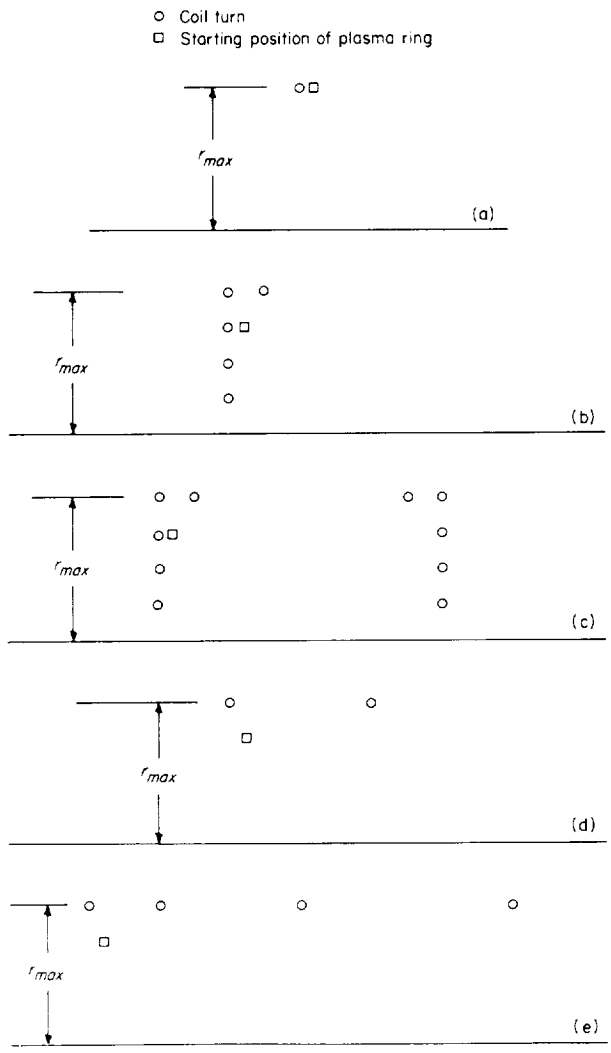

(a) Single-turn coil.
(b) Five-turn coil.
(c) Scylla type double coil.
(d) Two-coil, two-phase accelerator.
(e) Four-coil, two-phase accelerator.

FIGURE 2. Coil configurations used in computations.

RESULTS AND DISCUSSION

SINGLE-COIL ACCELERATOR

Some of the results obtained from the computation of the properties of a single-coil induced-electromotive-force accelerator are presented in figures 3 to 7 and in table I. The paths shown in figure 3 were obtained by using the initial condition that all velocities of the ring were zero at $\tau_0=0$. The results shown include two accelerators, one consisting of a single-turn coil (fig. 2(a)), and the other consisting of a five-turn coil (fig. 2(b)) which more or less simulates the current distribution used in the cup coil discussed in reference 5. The effects on the plasma-ring path of starting the ring motion at times τ_0 other than zero are shown in figure 4. The effects on the paths of adding a direct current to the single-coil accelerator are shown in figures 5(a) and 5(b). The variation of the logarithm of the nondimensional axial velocity $\dot{x}/\omega r_{max}$ with the logarithm of the drive intensity factor $I/\omega r_{max}$ is shown in figure 7.

The values presented in table I represent the maximum velocities computed for a single-coil accelerator using hydrogen, argon, and air plasmas.

Analysis of plasma paths. A study of the paths shown in figures 3(a) to 3(d) shows that the shapes of the paths of a given accelerator which start at $\tau_0=0$ are remarkably similar for a large range of values of $I/\omega r_{max}$ and n/r_{max} and that the paths themselves are smooth and proceed in a more or less forward direction. These path characteristics are of the type that can be considered to be desirable for an accelerator that is, forward motion and confinement to a radius roughly equal to that of the drive system.

The undesirable effects on the characteristics of paths obtained by starting the plasma ring at times τ_0 other than zero are seen in figure 4. The paths shown have a tendency to expand rapidly in the radial direction when $\frac{I}{\omega r_{max}}=0.0001$ (fig. 4(a)). When $\frac{I}{\omega r_{max}}=0.1$, the paths may be very erratic in that they reverse directions, loop around the drive coil, and finally escape in a direction completely foreign to the desired path (fig. 4(b)).

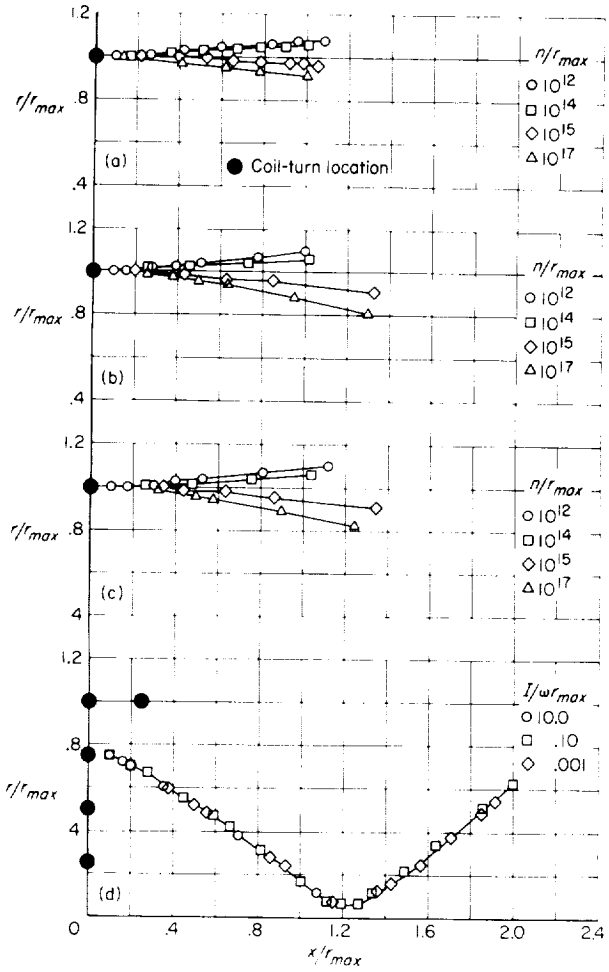

(a) Single-turn drive coil. $\frac{I}{\omega r_{max}}=0.001$.

(b) Single-turn drive coil. $\frac{I}{\omega r_{max}}=0.100$.

(c) Single-turn drive coil. $\frac{I}{\omega r_{max}}=100$.

(d) Five-turn drive coil. $\frac{n}{r_{max}}=10^{11}$.

FIGURE 3.– Effect of changing the values of the parameters $I/\omega r_{max}$ and n/r_{max} on the paths of hydrogen plasma rings. Initial conditions: $\dot{x}_0=\dot{r}_0=\dot{\theta}_0=\tau_0=0$.

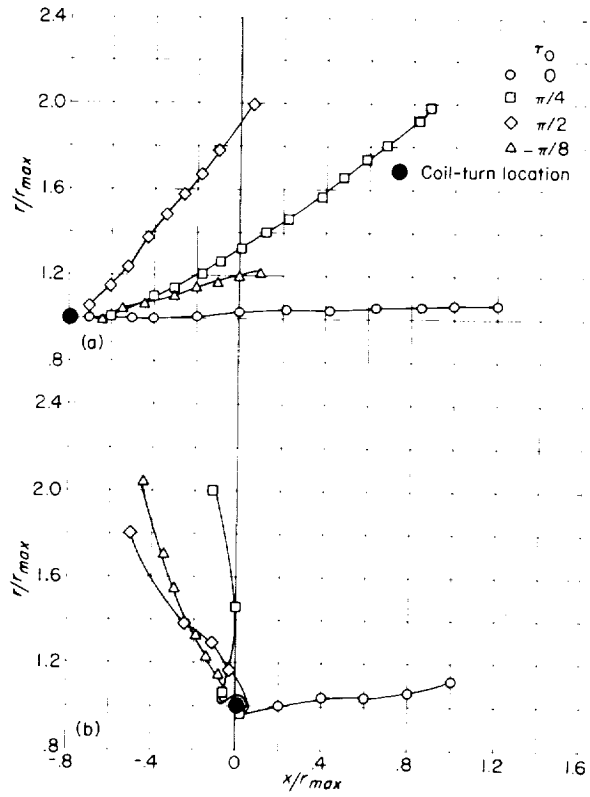

(a) $\frac{I}{\omega r_{max}}=0.0001$; $\frac{n}{r_{max}}=10^{11}$.

(b) $\frac{I}{\omega r_{max}}=0.1$; $\frac{n}{r_{max}}=10^{11}$.

FIGURE 4.– Paths of a hydrogen plasma ring in the field of a single-turn coil, showing effects of different starting times. Initial conditions: $\dot{x}_0=\dot{r}_0=\dot{\theta}_0=0$; $\frac{x_0}{r_{max}}=0.1$; $\frac{r_0}{r_{max}}=1.0$.

The divergence of the paths, particularly for $\frac{I}{\omega r_{max}}=0.1$, may be due to the effects of starting the ring in the presence of an existing magnetic field.

Other examples of erratic behavior are seen in figure 5, which shows some effects of starting a ring in the presence of a field caused by a steady current. These paths have irregularities and escape features similar to those in figure 4. The development of these effects with increasing value of the steady magnetic field is seen in figure 5(a). The effects of changing both the maximum value of the alternating current and the direct current together are shown in figure 5(b). It is interesting to note in figure 5(b) that, as $I/\omega r_{max}$ increases, the path irregularities and the rate of escape in the radial direction also increase. This behavior is more or less in agreement with the conditions observed in figure 4, where the path irregularities increase with increasing $I/\omega r_{max}$.

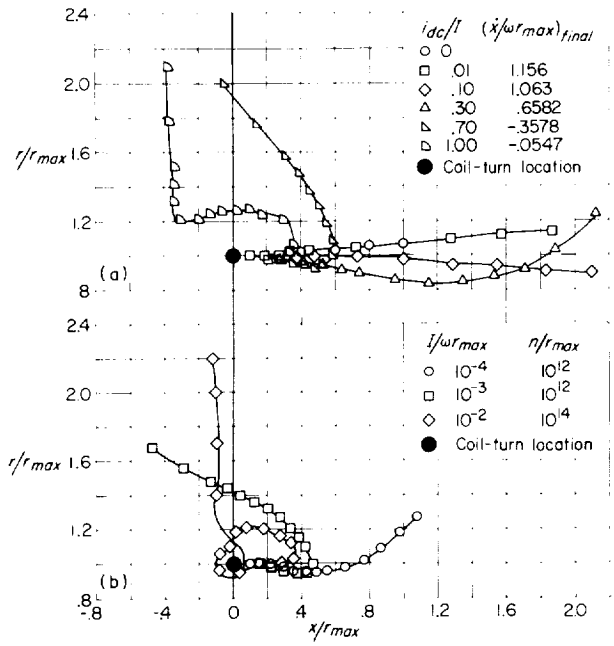

(a) $\frac{I}{\omega r_{max}}=0.001$; $\frac{n}{r_{max}}=10^{12}$.

(b) $I=i_{dc}$.

FIGURE 5.—Paths of a hydrogen plasma ring accelerated in a single-coil field, showing the effects of both a direct current and an alternating current flowing in the drive coil. Initial conditions: $\dot{x}_0=\dot{r}_0=\dot{\theta}_0=\tau_0=0$; $\frac{x_0}{r_{max}}=0.1$; $\frac{r_0}{r_{max}}=1.0$.

Some explanation of this erratic behavior may be seen by examination of figure 6 in which the variations of the computed values of r/r_{max} (or ρ), x/r_{max} (or χ), $\dot{x}/\omega r_{max}$ (or $\dot{\chi}$), $r\dot{\theta}_e/\omega r_{max}$ (or $\rho\dot{\phi}_e$), and γ_m with $\tau=\omega t$ are presented for the path shown in figure 5(a) for which $\frac{i_{dc}}{I}=1$. In order to interpret these graphs, it is to be noted that the axial acceleration from equation (19b) depends entirely on the product of $\rho\dot{\phi}_e$, γ_m, and $\partial\alpha_m/\partial\chi$; for this particular path, when $\dot{\phi}_{e,0}=\dot{\phi}_{i,0}=0$, $\dot{\phi}_i=-\frac{\dot{\phi}_e}{\beta}$ and hence is negligible. It is seen in figure 6 that $r\dot{\theta}_e/\omega r_{max}$ alternates in sign several times during the first quarter-cycle. Since both γ_m and $\partial\alpha_m/\partial\chi$ do not change sign, the acceleration must therefore change sign. The effect of the negative acceleration is seen from the first integration, the curve for $\dot{x}/\omega r_{max}$, to be sufficient to cause negative axial velocities to occur and even finally from the second integration, the curve for x/r_{max}, to cause the position of the ring to become negative.

The oscillation of the sign of $\dot{\phi}_e$, which caused this axial reversal, is dependent on the sign of the numerator of equation (19c) which for this path is $\rho\beta B[\rho\alpha_m(1+\sin\ \tau)-\rho\alpha_{m,0}]$. The effects of the motion are such that after some velocity is achieved the term α_m decreases faster than $(1+\sin\ \tau)$ increases and thus $\dot{\phi}_e$ becomes negative;

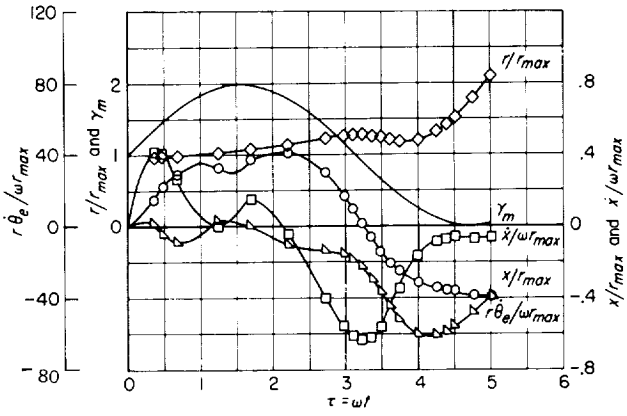

FIGURE 6.—Computed data for a hydrogen plasma ring accelerated in the magnetic field of a single-turn coil driven by both direct and alternating currents in which the value of the direct current equals the maximum value of the alternating current. Starting conditions: $\frac{x}{r_{max}}=0.1$; $\frac{r}{r_{max}}=1.0$; $\dot{x}_0=\dot{r}_0=\dot{\theta}_0=\tau_0=0$. $\frac{I}{\omega r_{max}}=0.001$; $\zeta=0.001$; $i_{dc}=I=1$; $\beta=1,845$.

the acceleration is thereby reversed and also the velocity is reduced. This reduction, however, allows $\alpha_m(1+\sin\tau)$ to become greater than $\alpha_{m,0}$ and, again, $\dot{\phi}_r$ becomes positive. In this fashion then the oscillation in $\rho\dot{\phi}_r$ occurs. If $\alpha_{m,0}$ is zero, as in the paths shown in figure 3, then these reversals of sign do not occur and the acceleration proceeds forward in a regular fashion. Also, reducing the values of $I/\omega r_{max}$ reduces these erratic effects (fig. 5(b)). Such a reduction occurs because the change in χ during a cycle is small so that α_m does not change so rapidly; the undesired oscillation of $\dot{\phi}_r$ is thereby slowed down or stopped with the result that the erratic behavior seen in the strong field paths is greatly reduced.

This reversal effect is somewhat surprising inasmuch as a plasma ring is generally expected to move from the stronger to the weaker portion of the magnetic field. Further study and perhaps some experimentation are required to show whether this phenomenon actually exists or is characteristic only of the motion of a single ring in a combined alternating and steady magnetic field. Some importance could be attached to this phenomenon inasmuch as it is directly associated with the problem of inserting a plasma into a mirror machine or other direct-current containment machinery with the use of a single-coil accelerator.

These considerations concerning plasma-ring paths indicate that the ring should start immediately ahead of the coil with a value of $I/\omega r_{max}$ not much greater than 0.0001, if a reasonable jet-like plasma stream is desired from the accelerator, and that superimposed steady magnetic fields will most likely not be beneficial to the containment of the plasma ring within the radius of the drive-coil system.

Analysis of maximum velocity values.—The maximum values of the four nondimensional velocities computed for a single-coil accelerator using hydrogen, argon, and air plasmas are presented in table I to show the orders of magnitude of these velocities. For example, the ratio of the electron azimuthal velocity to the ion azimuthal velocity is nearly equal to the value of β. A large variation is noted in the ratio of the axial velocity of the ring to the azimuthal ion velocity, from about 80 to roughly 2,000. On the other hand, the ring axial velocity varies from 0.1 to 0.03 of the electron azimuthal velocity.

The maximum axial velocities exhibit several important features which are better observed in figure 7. The curves shown in this figure are composed of two straight lines, with a transition between the two that is almost a sharp break. The slope of the curve is found to be very close to 1 for small values of $I/\omega r_{max}$ and close to $\frac{1}{2}$ for large values of $I/\omega r_{max}$. From these values, the axial velocity may be expressed by the following two relations:

$$\frac{\dot{x}}{\omega r_{max}} = C_1\sqrt{\frac{I}{\omega r_{max}}} \qquad \left(\frac{I}{\omega r_{max}} > C\right) \tag{20}$$

and

$$\frac{\dot{x}}{\omega r_{max}} = C_2\frac{I}{\omega r_{max}} \qquad \left(\frac{I}{\omega r_{max}} < C\right) \tag{21}$$

where C is the value of $I/\omega r_{max}$ at the knee of the curve.

An examination of the basic computed data showed that the knee of the curve occurs at values of $I/\omega r_{max}$ which accelerate the plasma ring away from the vicinity of the drive coil in 0.25 to 0.50 of a drive-current cycle. Thus, equation (20) may

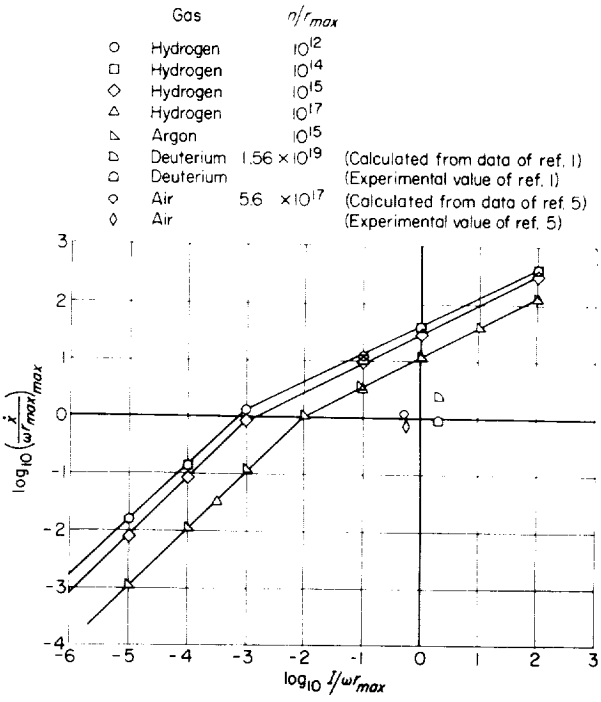

FIGURE 7. Effects of varying $I/\omega r_{max}$ and n/r_{max} on the maximum velocity of various plasma rings accelerated in a single-turn field. Initial conditions: $\dot{x}_0$ $\dot{r}_0$ $\dot{\theta}_0$ τ_0 0.

TABLE I.—MAXIMUM VALUES OF THE VARIOUS VELOCITIES COMPUTED FOR A SINGLE-COIL INDUCED-ELECTROMOTIVE-FORCE ACCELERATOR

Drive intensity, $I/\omega r_{max}$	Ions per unit length, n/r_{max}	Nondimensional axial velocity, $\dot{x}/\omega r_{max}$	Nondimensional radial velocity, $\dot{r}/\omega r_{max}$	Nondimensional electron azimuthal velocity, $r\dot{\theta}_e/\omega r_{max}$	Nondimensional ion azimuthal velocity, $r\dot{\theta}_i/\omega r_{max}$
Single-turn coil; hydrogen plasma					
10^{-5}	10^{12}	0.0136	0.001263	0.392	−0.00027
	10^{15}	.007884	−.0004029	.2251	−.000122
10^{-4}	10^{12}	.1536	.01414	6.90	−.00374
	10^{14}	.1389	.008117	5.285	−.00286
	10^{15}	.08299	−.003786	1.715	−.000929
	10^{17}	.009588	−.001173	−.03446	−.0000187
10^{-3}	10^{12}	1.136	.1095	32.00	−.0175
	10^{15}	.7939	−.06520	13.71	−.0074
	10^{17}	.1037	−.01150	.2766	−.0001499
10^{-1}	10^{12}	12.61	1.188	330	−.1788
	10^{14}	11.97	.5766	293.7	−.159
	10^{15}	9.825	−1.150	147.1	−.0797
	10^{17}	3.316	−.704	6.23	−.00337
1.0	10^{12}	40.79	3.667	1,040	−.564
	10^{14}	38.82	1.659	895.4	−.485
	10^{15}	30.73	−3.403	464.7	−.2519
	10^{17}	10.50	−2.174	19.88	−.01071
100	10^{12}	400.5	37.49	10,477	−5.676
	10^{14}	380.2	18.06	9,031	−5.027
	10^{15}	311.9	−36.95	4,532	−2.456
	10^{17}	106.1	−22.59	192	−.1038
Single-turn coil; argon plasma					
10^{-5}	10^{15}	0.001270	−0.00007281	−0.1558	0.000002141
10^{-4}	10^{15}	.0127	−.000726	1.505	−.0000206
10^{-3}	10^{15}	.1413	−.00666	21.79	−.000300
10^{-2}	10^{15}	1.102	−.1140	110.1	−.001532
10^{-1}	10^{15}	3.976	−.5310	367.9	−.00508
1	10^{15}	12.78	−1.795	1,171	−.01608
100	10^{15}	128	−18	11,650	−.156
Five-turn coil; air plasma					
0.0227	5.6×10^{17}	0.346	−0.330	2.42	−0.0000452
.117	5.6×10^{17}	1.106	−1.17	6.541	−.0001223
.568	5.6×10^{17}	2.613	−2.815	14.98	−.0002801

be expected to result from the assumption of a linear increase in the drive current; that is, the acceleration occurs during the period for which $\sin \tau \approx \tau$. Equation (21) results from the integrated effect of a large number of drive-current cycles acting on the ring during the period of acceleration. In fact, a highly approximated solution involving these conditions can be effected to show a theoretical basis for equations (20) and (21). (See appendix A.)

Approximate equation for estimation of axial velocity.—Two expressions which may be used for the estimation of the axial velocities obtained in a single-coil plasma accelerator are given by equations (A7) and (A10) which are developed in the appendix. These relations are

$$\frac{\dot{x}}{\omega r_{max}} = k_1 \left[\frac{\rho}{(\rho+2\zeta)\beta}\right]^{1/4} \left(\frac{I}{\omega r_{max}}\right)^{1/2}$$

for large values of $I/\omega r_{max}$ and

$$\frac{\dot{x}}{\omega r_{max}} = k_2 \left[\frac{\rho}{(\rho+2\zeta)\beta}\right]^{1/2} \frac{I}{\omega r_{max}}$$

for small values of $I/\omega r_{max}$. The coefficients k_1 and k_2 are assumed to be constants equal to the average

effect of the magnetic field on the plasma ring. Because of the complications involved in the calculations of k_1 and k_2, it is preferable to determine the values from computed data, such as those given in table I. If k_1 and k_2 are determined from the hydrogen data for $\frac{I}{\omega r_{max}}=100$ and $\frac{I}{\omega r_{max}}=10^{-4}$, the values of k_1 will vary from 260 to 268 for the range of the given values of ζ, whereas the values of k_2 will vary from 58,000 to 66,000 for the same values of ζ. If the average values of k_1 and k_2 are used with $\rho \approx 1$, then equation (A7), for large values of $I/\omega r_{max}$, may be expressed as

$$\frac{\dot{x}}{\omega r_{max}}=263\left[\frac{1}{(1+2\zeta)\beta}\right]^{1/4}\left(\frac{I}{\omega r_{max}}\right)^{1/2} \qquad (22)$$

and equation (A10), for small values of $I/\omega r_{max}$, as

$$\frac{\dot{x}}{\omega r_{max}}=62{,}900\left[\frac{1}{(1+2\zeta)\beta}\right]^{1/2}\frac{I}{\omega r_{max}} \qquad (23)$$

The transfer point between the two equations occurs for values of $I/\omega r_{max}$ at which $\dot{x}/\omega r_{max}$ is approximately equal to 1. (See fig. 7.) It should be noted that the foregoing values of k_1 and k_2 are developed for a single-turn, single-coil accelerator. (See fig. 2(a).) Other single-coil configurations with plasma rings starting at different locations will most likely have different values for k_1 and k_2.

The applicability of these equations to a gas other than hydrogen (for example, argon) may be checked by substituting 72,784, the value of β for argon, into equations (22) and (23) and then comparing the results with the corresponding computed values given in table I. If $\frac{I}{\omega r_{max}}=100$, the value obtained by use of equation (22) is 127.6 as compared with 128, the value from table I; if $\frac{I}{\omega r_{max}}=10^{-4}$, the value from use of equation (23) is 0.0134 as compared with 0.0127 from table I. This close agreement may be fortuitous, but it does suggest that the foregoing relations should be useful in the comparison of various accelerators or for the extrapolation of the results obtained from a given accelerator, provided values of k_1 and k_2 that are representative of the particular accelerator used can be determined.

Comparison of theory with experiment. - Experimental values of axial velocities obtained in single-coil accelerators are reported in references 1 and 5. These values may be used for comparison with values computed from equation (22). Consider the data given in reference 1, for which circuit capacity is 0.88 microfarad; the total inductance is 0.295 microhenry, the ring mass is 13×10^{-6} gram of deuterium, the driving voltage is 60,000 volts, and the final velocity is 5×10^6 centimeters per second. The values of the parameters used in this paper, when calculated from these data, are as follows:

$$\frac{I}{\omega r_{max}}=1.051$$

(with the assumption that one-half of the drive current is used to drive the forward-moving plasma ring and one-half to drive the rearward-moving plasma ring)

$$\frac{n}{r_{max}}=1.56\times10^{19} \text{ or } \zeta=15{,}600$$

$$\beta=3{,}690$$

(with the assumption of singly ionized deuterium ions).

If these values of ζ, β, and $I/\omega r_{max}$ are substituted into equation (22), the resultant value of $\dot{x}/\omega r_{max}$ is about 2.5, which may be compared with the experimental value of 0.919.

A similar analysis may also be made of the data presented in reference 5. The values of the parameters $I/\omega r_{max}$, ζ, and β obtained from these data are

$$\frac{I}{\omega r_{max}}=0.587$$

$$\frac{n}{r_{max}}=5.75\times10 \text{ or } \zeta=575$$

$$\beta=53{,}500$$

(with the assumption that the average molecular weight for air is 29).

If these values are substituted into equation (22), the resultant value of $\dot{x}/\omega r_{max}$ is 2.05. However, the single-turn coil on which equation (22) is based is appreciably different from the cup coil of reference 5. The five-turn coil (fig. 2(b)) has a current distribution which is fairly representative of the current distribution found in the single-turn cup-shape coil used. Actual computations of the five-turn coil, using equation (22), with $\frac{I}{\omega r_{max}}=0.117$, gave a value for $\dot{x}/\omega r_{max}$

of 1.106. The reduced value of $I/\omega r_{max}$ was used to keep the total current flowing around the five-turn coil the same as the current flowing in the cup coil.

MULTIPLE-COIL SYSTEMS

Computations were also made of the motion of a hydrogen plasma ring in the magnetic fields created by several commonly used multiple-coil devices. The first system was a magnetic-mirror system similar in operation to the Scylla fusion machine discussed in reference 3. The second system consisted of a two-coil traveling-wave system in which the drive current of the second coil lagged that of the first by $\pi/2$ radians. The third system was an extension of the second in that two more turns were added in which the phase lags were π and $3\pi/2$ radians, respectively. Even though the studies were incomplete, they did show several interesting phenomena concerning the motion of plasma rings in multiple-coil systems.

Two-coil fusion machine (Scylla).—The system used for this computation consisted of two coils located as shown in figure 2(c) and was investigated to determine the existence of plasma-ring motion which would be symmetrical with respect to a center plane between the coils and oscillatory with respect to time. Several of the paths computed are shown in figure 8. All the paths started at $x=-0.9$ and $\rho=0.75$. Although many of the paths turn around and start back, the reversal itself is not symmetrical and the paths do not retrace themselves, so that no evidence of periodicity seems to exist. Thus, this system does not show evidence that it is capable of holding a plasma ring in an oscillating path for more than a cycle or two. The results of the computations suggest that this system has very poor plasma-containment features.

Two-phase traveling-wave accelerators.—The two-coil, two-phase system used for an initial survey is shown in figure 2(d). The four-coil system, obtained by extending the two-coil system, is shown in figure 2(e). The paths obtained for the two-coil, two-phase, traveling-wave system for a range of values of $I/\omega r_{max}$ are shown in figure 9. These paths show that the two-coil system may have poor confinement properties, as only one of the paths computed remains within the radius of the system throughout the acceleration period.

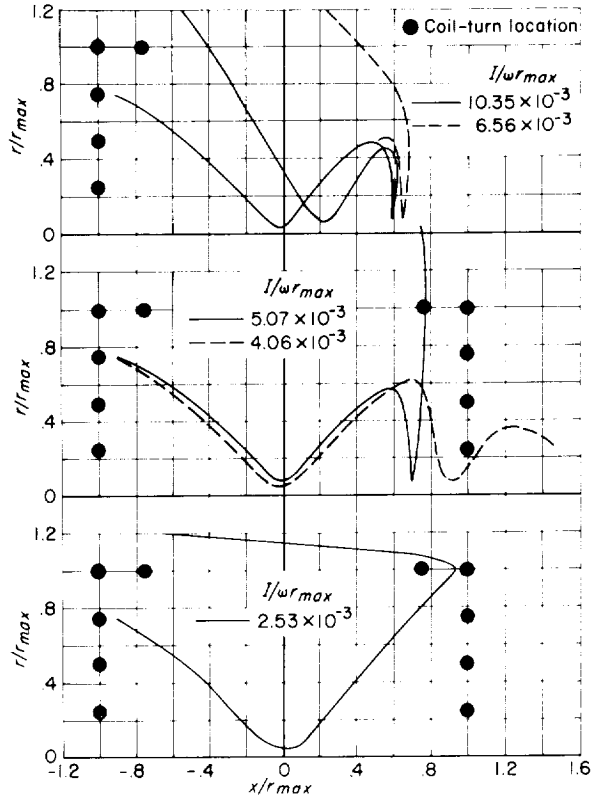

FIGURE 8.—Paths of a hydrogen plasma ring in a double-coil field similar to that of the Scylla fusion machine. Initial conditions: $\dot{x}_0=\dot{r}_0=\dot{\theta}_0=\tau_0=0$.

This behavior would indicate that the range of values of $I/\omega r_{max}$ for which even a simple traveling-wave accelerator will operate as a linear accelerator is quite limited. A similar condition is observed for the paths in the four-coil, two-phase, traveling-wave accelerator presented in figure 10. Again, only one of the paths considered remained within the confines of the accelerator.

The complete data on the confined path for the four-coil accelerator $\frac{I}{\omega r_{max}}=3.16\times10^{-4}$ is shown in figure 11. Two interesting features are observed in this figure: one is that the electron velocity $\frac{r\dot{\theta}_e}{\omega r_{max}}$ is always positive, the other is that the ring time history does not lag the magnetic-field time history within the coil by more than one-fourth of a drive-current cycle (that is, $\pi/2$ radians). The time history of this confined path, $\frac{I}{\omega r_{max}}=3.16\times10^{-4}$, is compared in figure 12 with two paths for which the plasma ring escaped from the confines

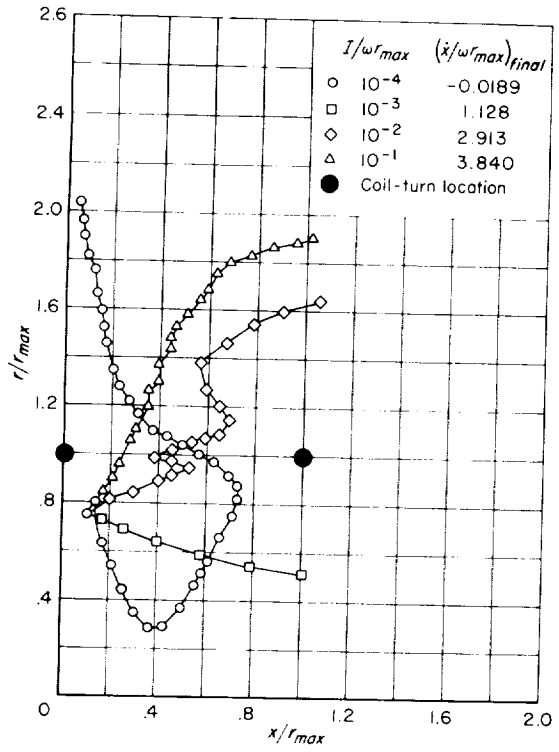

FIGURE 9.—Paths of a hydrogen plasma ring in a two-phase, traveling-wave magnetic field, showing the effects of varying the drive-intensity parameter $I/\omega r_{max}$. Initial conditions: $\dot{x}_0=\dot{r}_0=\dot{\theta}_0=\tau_0=0$; $\frac{n}{r_{max}}=10^{13}$.

of the accelerator, $\frac{I}{\omega r_{max}}=1.00\times10^{-3}$ and 3.16×10^{-3}. It is seen that, for both paths for which the ring escapes, the ring time history leads the magnetic-field time history, so that the plasma ring may be advancing into a magnetic field opposite in sign to that in which the ring is formed. This behavior is believed to give rise to the reactions which lead to the escape of the ring. Also, if the ring slips more than a half-cycle (that is, phase lags occur greater than π), it is reasonable to suppose that similar nonconfining reactions will occur.

Although this analysis represents idealized plasma rings moving through a vacuum, it is difficult to see that an actual traveling-wave accelerator would be any less stringent in its design requirements. It is believed, therefore, that care must be taken in choosing the correct values of the parameters $I/\omega r_{max}$, ζ, and β if a

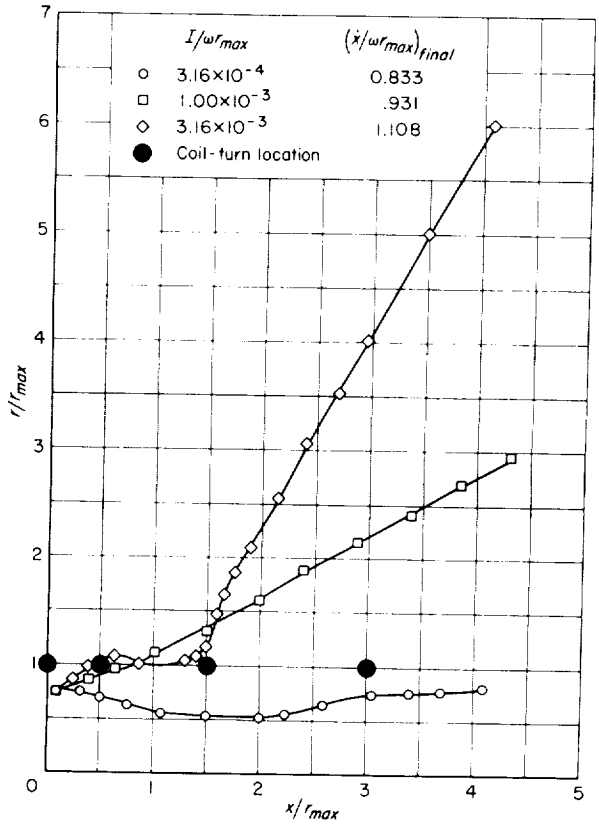

FIGURE 10.—Paths of a hydrogen plasma ring accelerated in a four-coil, two-phase, traveling-wave system showing the effects of varying the drive-intensity parameter $I/\omega r_{max}$. Initial conditions: $\dot{x}_0=\dot{r}_0=\dot{\theta}_0=\tau_0=0$; $\frac{n}{r_{max}}=10^{13}$.

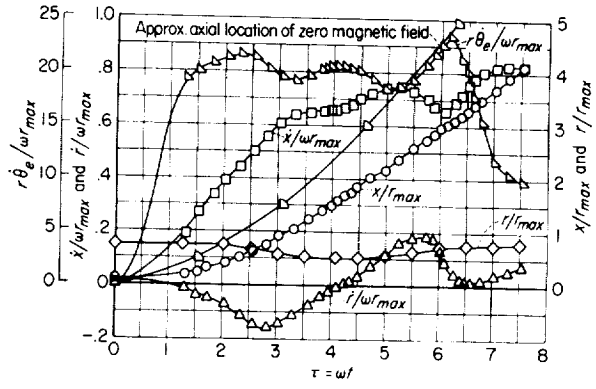

FIGURE 11.—Computed data for a hydrogen plasma ring accelerated in a four-coil, two-phase, traveling-wave accelerator. Coil radius $=r_{max}$; coil locations: 0, $0.5r_{max}$, $1.5r_{max}$, and $3.0r_{max}$; initial conditions: $\dot{x}_0=\dot{r}_0=\dot{\theta}_0=\tau_0=0$.

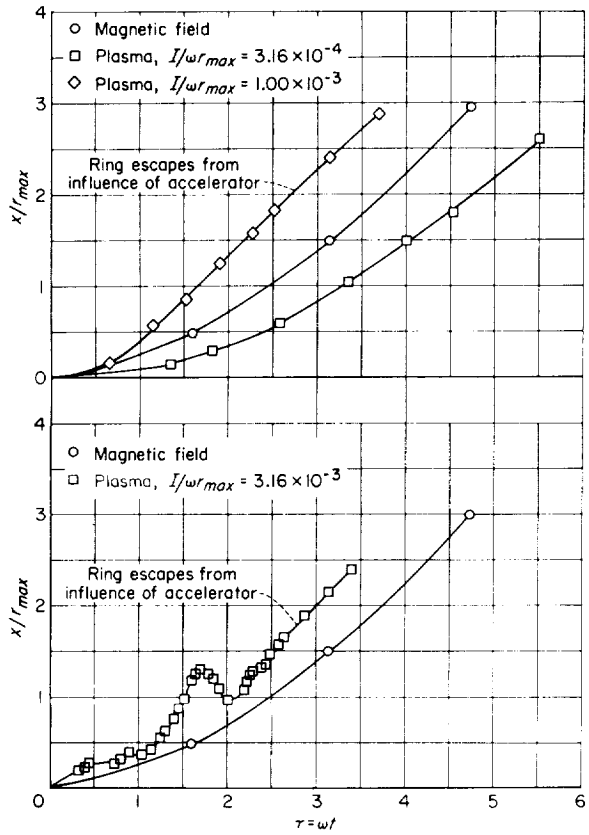

FIGURE 12.—Comparison of time history of x-coordinate of a plasma ring accelerated in a four-coil, two-phase accelerator with the axial time history of the magnetic field. Initial conditions: $\dot{x}_0 = \dot{r}_0 = \dot{\theta}_0 = 0$; $\frac{r_0}{r_{max}} = 0.75$.

traveling-wave accelerator is to keep a ring confined within its radius during the entire acceleration period.

CONCLUDING REMARKS

The equations for the analysis of the motion of an idealized plasma ring under the influence of a changing magnetic field show that three parameters control the motion of the plasma ring in a given system under given initial conditions. These parameters are the ratio of the maximum drive current to the product of the drive frequency in radians and the maximum radius of the drive-coil system, the ratio of the number of electrons or ions in the ring to the maximum radius of the drive coil, and the ratio of the mass of the ions composing the ring to the corresponding mass of the electrons.

The computed results indicate that a single-turn, single-coil accelerator should function best if the plasma is allowed to form just ahead of the coil and to accelerate from that position. The paths of rings which started in the presence of a magnetic field usually became erratic and escaped from the confines of the accelerator in more or less a radial direction.

Equations are given which allow the approximate prediction of the axial velocity obtained in a single-coil accelerator provided the velocity is known for some set of the control parameters. Comparison of the theoretical value with available experimental data showed reasonable agreement, better than to an order of magnitude.

A rather preliminary analysis of a traveling-wave accelerator indicated that this system may be expected to be sensitive to the values of the control parameters used; thus, a very sophisticated design will most likely be necessary if this accelerator is to be operated successfully.

LANGLEY RESEARCH CENTER,
NATIONAL AERONAUTICS AND SPACE ADMINISTRATION,
LANGLEY AIR FORCE BASE, VA., *July 12, 1961.*

APPENDIX A

APPROXIMATE EQUATIONS FOR THE AXIAL VELOCITY

An approximate integration of the equations of motion (19b) and (19c) can be made for the condition for which the velocity of the plasma ring is zero at the starting time τ_0 and the drive current is alternating only with the same value in each turn of the drive coil. Under these conditions the constants C_e and C_t in equation (19c) are zero. As a further simplification ρ is considered constant throughout the integration. This is a reasonably good approximation as illustrated in figures 3(a), 3(b), and 3(c). Moreover, the magnetic-vector-potential derivatives with respect to χ are assumed to act at constant average values throughout the more intense portion of the acceleration range—that is, between $\chi=0$ and $\chi=1.0$. Under these conditions equation (19c) may be written

$$\dot{\phi}_e \approx -\frac{B\left[\sum_{m=1}^{S}\alpha_m\right]_{av}}{\rho+2\zeta}\sin\tau \tag{A1}$$

with the assumption that $\beta\approx\beta+1$. This assumption is valid since the minimum value of β, that for hydrogen ion plasma, is 1,845. Equation (19b) may also, under these conditions, be written

$$\ddot{\chi} \approx -\frac{\rho B\dot{\phi}_e\left[\sum_{m=1}^{S}\frac{\partial\alpha_m}{\partial\chi}\right]_{av}}{\beta}\sin\tau \tag{A2}$$

If the following product is written as a constant D, or

$$D=-\left[\sum_{m=1}^{S}\alpha_m\right]_{av}\left[\sum_{m=1}^{S}\frac{\partial\alpha_m}{\partial\chi}\right]_{av}$$

then

$$\ddot{\chi}=\frac{\rho DB^2\sin^2\tau}{(\rho+2\zeta)\beta} \tag{A3}$$

This equation may be integrated once to give the following relation, where the constant of integration is equal to zero to satisfy starting conditions:

$$\dot{\chi}=\frac{\rho D}{\rho+2\zeta}\frac{B^2}{\beta}\left(\frac{\tau}{2}-\frac{\sin 2\tau}{4}\right) \tag{A4}$$

Equation (A4) may be conveniently treated for two drive currents: large drive currents for which the acceleration is so large that the process is completed in a short portion of the drive-current cycle, and small drive currents for which the acceleration is so small that the process involves many cycles and the term $\tau/2$ becomes much larger than the term $\sin 2\tau/4$.

LARGE ACCELERATION

If the acceleration is large, the $\sin 2\tau$ term may be eliminated with the substitution of $2\tau-8\tau^3/6$ into equation (A4). Then,

$$\dot{\chi}=\frac{\rho DB^2}{(\rho+2\zeta)\beta}\frac{\tau^3}{3} \tag{A5}$$

This expression may be integrated once to give

$$\chi=\frac{\rho DB^2\tau^4}{12\beta(\rho+2\zeta)} \tag{A6}$$

The elimination of τ between equations (A5) and (A6) results in the following relation:

$$\dot{\chi}=\frac{12^{3/4}}{3}\left(\frac{\rho D}{\rho+2\zeta}\right)^{1/4}\frac{B^{1/2}}{\beta^{1/4}}\chi^{3/4}$$

The basic computations showed that the maximum velocity was attained at values of χ about equal to 1.0. With this assumption and the substitution for B of equation (15), the velocity in the x-direction for large values of $I/\omega r_{max}$ can be written

$$\dot{\chi}=k_1\left[\frac{\rho}{(\rho+2\zeta)\beta}\right]^{1/4}\left(\frac{I}{\omega r_{max}}\right)^{1/2} \tag{A7}$$

where k_1 is a constant involving the coil configuration of the particular accelerator.

Equation (A7) agrees with the empirical relation (20) and thereby the assumptions made in this analysis are justifiable within limits.

SMALL ACCELERATION

If equation (A4) is considered for a small acceleration (that is, $I/\omega r_{max}$ is small), then it is seen that the contribution of the term sin $2\tau/4$ is small compared with that of the term $\tau/2$. Thus, the equation for $\dot{\chi}$ may be approximated by

$$\dot{\chi} \approx \frac{\rho D}{\rho+2\zeta} \frac{B^2}{\beta} \frac{\tau}{2} \tag{A8}$$

This equation may be integrated to give

$$\chi = \frac{\rho D B^2}{4(\rho+2\zeta)\beta} \tau^2 \tag{A9}$$

Again, in both equations the constants of integration are set equal to zero to satisfy the initial conditions $\dot{\chi}_0 = \chi_0 = \tau_0 = 0$. If the time τ is eliminated from equations (A8) and (A9) and B is expressed in terms of $I/\omega r_{max}$, then the equation for the axial velocity for small values of $I/\omega r_{max}$ may be written

$$\dot{\chi} = k_2 \left[\frac{\rho}{(\rho+2\zeta)\beta}\right]^{1/2} \frac{I}{\omega r_{max}} \tag{A10}$$

where k_2 is a constant involving the coil configuration of the particular accelerator.

This equation is in agreement with the empirically observed equation (21) and indicates that the assumptions made are also reasonable for small accelerations.

REFERENCES

1. Marshall, John: Acceleration of Plasma Into Vacuum. Proc. Second United Nations Int. Conf. on Peaceful Uses of Atomic Energy (Geneva), vol. 31—Theoretical and Experimental Aspects of Controlled Nuclear Fusion, 1958, pp. 341–347.
2. Boyer, K., Hammel, J. E., et al.: Theoretical and Experimental Discussion of Ixion, a Possible Thermonuclear Device. Proc. Second United Nations Int. Conf. on Peaceful Uses of Atomic Energy (Geneva), vol. 31—Theoretical and Experimental Aspects of Controlled Nuclear Fusion, 1958, pp. 319–324.
3. Elmore, W. C., Little, E. M., and Quinn, W. E.: Neutrons From Plasma Compressed by an Axial Magnetic Field (Scylla). Proc. Second United Nations Int. Conf. on Peaceful Uses of Atomic Energy (Geneva), vol. 32—Controlled Fusion Devices, 1958, pp. 337–342.
4. Ziemer, Richard W.: Experimental Magneto-Aerodynamics. [Preprint] 707–58, American Rocket Soc., Nov. 1958.
5. Matthews, Clarence W., and Cuddihy, William F.: Experimental Study of a Single-Coil Induced-Electromotive-Force Plasma Accelerator. NASA TN D-639, 1961.
6. Harnwell, Gaylord P.: Principles of Electricity and Electromagnetism. Second ed., McGraw-Hill Book Co., Inc., 1949.

U.S. GOVERNMENT PRINTING OFFICE: 1962

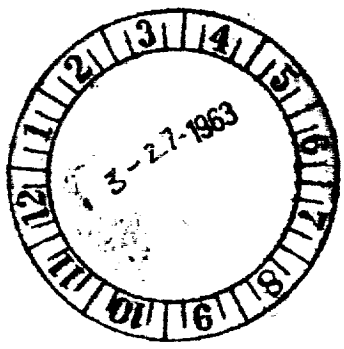
3-27-1963